Shahrood University of Technology
Iranian Society of Mining Engineering (IRSME)
Journal of Mining and Environment (JME)
journal homepage: www.jme.shahroodut.ac.ir
THOMSON REUTERS

Vol. 11, No. 1, 2020, 63-76.
DOI: 10.22044/jme.2019.7980.1667.

Bayesian Data Fusion: a Reliable Approach for Descriptive Modeling of Ore Deposits

B. Tokhmechi[1*], S. Ebrahimi[2], H. Azizi[3], S.R. Ghavami-Riabi[1], and N. Farrokhi[4]

1. Faculty of Mining, Petroleum & Geophysics Engineering, Center of Excellency in Mining Engineering, Shahrood University of Technology, Shahrood, Iran
2. Faculty of Mining, Petroleum & Geophysics Engineering, Shahrood University of Technology, Shahrood, Iran
3. School of Electrical Engineering and Computer Sciences, University of North Dakota, Grand Forks, North Dakota, USA
4. Department of Cell & Molecular Biology, Faculty of Life Sciences & Biotechnology, Shahid Beheshti University, Tehran, Iran

Received 16 January 2019; received in revised form 3 April 2019; accepted 12 April 2019

Keywords

Data Assimilation
Complexity
Decision-making
Economic Geology
Uncertainty Reduction

Abstract

Recognition of ore deposit genesis is still a controversial challenge for economic geologists. Here, this task was addressed by the virtue of Bayesian data fusion (BDF), implementing available proofs: semi-schematic examples with two (Cu and Pb + Zn) and three (Cu, Pb + Zn, and Ag) evidences. The data, in the current paper being just concentrations of the indicated elements, was collected from the Angouran deposit in Iran at the prospecting and general exploration stages. BDF was used for discrimination between the three geneses of Massive Sulfide, Mississippi, and SEDEX types. A better genesis recognition with clear discrimination between the geneses was achieved by BDF, as compared to the earlier studies. The results obtained showed that uncertainties were reduced from 50% to less than 30%, and deposit recognition was greatly improved. Furthermore, we believe that using more properties can have a beneficial effect on the overall outcome. The comparison made between 2 and 3 properties showed that the amount of probable belonging values to any type of deposit was greater in 3 properties. It was also confirmed that using the completed information from the various stages of exploration progress can be amplified and be used for genesis recognition via BDF.

1. Introduction

Identification of the ore deposit genesis, one of the main duties of economic geologists, is an important step in exploration, surveying, sampling, and reserve modeling. For a proper identification, as proposed elsewhere [1-5], numerous information databanks, as listed below, needs to be put in place. The necessary information are the tectonic regime (magma tekton), mineral host rock and age, alteration or metasomatic zones of mineral host rock by hydrothermal or magmatic fluids, overall figure of the deposit (e.g. vein, layer, mass, porphyry), mineralization tissue (how deposit is placed in the host rock such as dispersed, massive or vein types), ore and gangue mineral (mineralization, *e.g.* iron, which might be as oxide, carbonate or sulfide as well as type of gangue), grade and ore deposit tonnage, and physico-chemical properties of fluid or magma (fluid inclusion and sustainable isotopes such as H, C, O, and S studies).

In the earlier methodologies, the use of a univariate data analysis to explore ore deposit genesis was common. As a result, the researcher could have ignored vast amounts of information and existing complexities, leading to probable misinterpretation and poor comprehension of what has happened

Corresponding author: tokhmechi@ut.ac.ir (B. Tokhmech).

during the course of genesis [6-13]. In contrast, the shift towards multivariate analysis approaches such as pattern recognition via genesis classification [14], mapping neural network [15], dynamic clustering [16], and hybrid clustering [17] has revolutionized our view towards recognition of ore deposit genesis. Nevertheless, even in the case of multivariate analysis, the resulting information is heavily dependent on the implemented statistical approach. This so-called fuzzy genesis recognition can be misleading; raising questions in regards to uncertainties, and how to obtain more reliable information out of the considered evidences.

A relatively new concept in geoscience is the use of sensor data fusion, with earliest applications in military cases towards promoting machine-human relationship and reducing uncertainties in reliable decisions. Data fusion has found its merits in other sciences [18, 19] through gathering more data from varieties of sensors [20-23]. Such improvements have allowed optimization of computational efficiency, removal of data redundancy, reduction of uncertainties and cost, improving the resolution for signal-to-noise ratio, and achieving more reliable and comprehensive results.

Pattern fusion, which is the integration in the level of decision, is the highest level of data fusion [18, 23]. In this paper, BDF was used for identification of schematic ore deposit genesis. It was assumed that three geneses might be considered for a deposit: Massive Sulfide, Mississippi, and SEDEX. The characteristics of these deposits are summarized in Table 1. The role of data fusion is to amplify the most possible genesis for a certain deposit. The results obtained were compared with the common methods to give a clear view of the benefits for the applied method.

Table 1. Brief characteristics of the MVT, SEDEX, and VMS (Besshi) type deposits.

Type deposit	Host rock	Alteration	Form	Texture	Ore minerals	Gangue minerals	Main Metals	Second metals	References
MVT	Carbonate-Dolomite	Dolomitization	Strataband-Stratiform	Disseminated, Veinlets	Galena, Sphalerite, Pyrite, Marcasite	Fluorite, Barite, Calcite, Quartz	Pb-Zn	Cu-Ba-F (Cu=0.001 to 0.05%) (Ag=1 to 40 ppm)	[11, 24]
SEDEX	Sedimentary-Volcanic rocks	Dolomitization-Solidification-Sericitization	Strataband, Stratiform-Tabular lenses-	Massive and fine Banded, Breccia, Disseminate	Galena, Sphalerite, ChalcoPyrite, Pyrite, Pyrrhotite	Calcite, Barite, Quartz, Dolomite	Zn-Pb-(Cu=0.05 to 0.5 %)	Mn-Fe, Mg-As-Sb-Tl (Ag= 6 to 250 ppm)	[11, 25]
VMS (Besshi)	Volcanic-Sedimentary	The Host Rock Metamorphism	Stratiform-Lenticular	Massive-Disseminated-Stockwork-Brecciated	Sphalerite, Galena, Pyrite, ChalcoPyrite, Pyrrhotite, ArsenoPyrite	Quartz, Calcite, Barite	Zn-Pb-(Cu=0.5 to 5%)	Ti-Au-Bi- Mg-Mn (Ag=2 to 90 ppm)	[11, 26]

2. Bayesian Data Fusion (BDF)

Conditional probability is the basis of BDF. The Bayes law [19, 23] is:

$$P(B|A)=\frac{P(A|B)P(B)}{P(A)} \quad (1)$$

in which $P(A|B)$ is a priori probability, $P(B)$ is the likelihood function, and $P(A)$ is a normalization factor. $P(B|A)$, the posteriori probability, is an indicator of the correctness of proposition of *B*. The result of the conditional probability $P(A|B)$ is in the range of [0, 1]. One means absolute belief to correctness of *A* when *B* is known. $P(A|B)$ is equal to zero when A is absolutely incorrect and *B* is known.

Suppose that *n* properties *of* S_1 to S_n are *n*-measured values from X_1 to X_n. There is a conditional probability for uncertainty as property of S_i, which is introduced by the X_i value. The likelihood function would be the first parameter to be calculated in the Bayesian algorithm:

$$L(X_i|Y)=\frac{P(X_i|Y)}{P(X_i|\neg Y)} \quad (2)$$

The Priori estimation can be calculated as:

$$O(Y)=\frac{P(Y)}{P(\neg Y)} \quad (3)$$

where $P(Y)$ and $P(\neg Y)$ are the probability of occurrence and non-occurrence *Y*, respectively. *O(Y)* represents the odds of the event. Posteriori estimation of proposition *Y* equals to:

$$O(Y|X_1,X_2,...,X_n)=O(Y)\times\prod_{i=1}^{n}L(X_i|Y) \quad (4)$$

where the likelihood functions and priori estimation are calculated by Equations 2 and 3, respectively. Posteriori probability (*Y*) in the case of knowing X_1 to X_n is equal to:

$$P(Y \mid X_1, X_2, ..., X_n) = \frac{O(Y \mid X_1, X_2, ..., X_n)}{1 + O(Y \mid X_1, X_2, ..., X_n)} \quad (5)$$

Suppose that there are two properties; if the properties were measured in two individual times, then the equation would be modified as follows [27]:

$$P(x \mid Y_1^1 Y_1^2) = \frac{P(x \mid Y_1^1) P(Y_1^1 \mid Y_0^1)}{P(x \mid Y_0^1)} \cdot \frac{P(x \mid Y_1^2) P(Y_1^2 \mid Y_0^2)}{P(x \mid Y_0^2)} \cdot \frac{P(x \mid Y_0^1 Y_0^2)}{P(Y_1^1 Y_1^2 \mid Y_0^1 Y_0^2)} \cdot \frac{P(x \mid Y_1^1) P(x \mid Y_1^2) P(x \mid Y_0^1 Y_0^2)}{P(x \mid Y_0^1) P(x \mid Y_0^2)} \times Normalization\ Factor \quad (6)$$

In the case of having three properties or more, Equation 6 will be modified based on 7 [27]:

$$P(x \mid Y_1^1 Y_1^2 Y_1^3) = \frac{P(x \mid Y_1^1) P(x \mid Y_1^2) P(x \mid Y_1^3) P(x \mid Y_0^1 Y_0^2 Y_0^3)}{P(x \mid Y_0^1) P(x \mid Y_0^2) P(x \mid Y_0^3)} \times Normalization\ Factor \quad (7)$$

Summation of $P(x \mid Y_1^1 Y_1^2)$ has to be equal to one, achieved with the normalization factor. To describe the procedure, an example is solved in Section 4.

3. Problem Definition

The knowledge about ore deposit genesis would, of course, put miners in great advantage in terms of cost reduction. Thus implementing proper exploratory techniques will save us the benefits of doubts during decision-making. During the last half century or so, varieties in the exploration techniques have been developed to be used in mines and further optimized [28-31].

Since characteristics of deposits are unique (see Table 2, for example), an identical genesis pattern for each is expected, which makes the identification process associated with great amounts of uncertainties. To be clear, in Figure 1, three triangles are extracted from the information in Table 2, which displays similarity between the numbered deposits and three well-known geneses of sulfide deposits, *i.e.* Mississippi Valley (MV), Massive Sulfide (MS), and SEDEX (S). In Figure 1, concentrations of the characteristic elements in MVT, SEDEX, and VMS are displayed, where the numbers correspond to the deposit values in Table 2. Centers of different panels in Figure 1 are considered as the absolute uncertainty point (33.3% membership to three genesis types). Accordingly, in places within Table 2, where the values for metal contents are missing, a spot has appeared in the middle of triangle (Figure 1), *i.e.* considered as a dummy spot. Location of the circles and square in all panels in Figure 1 are assigned based on the analysis of Cu, Zn + Pb, and Ag, respectively.

Often evidences are present that approve and simultaneously reject belonging of a deposit to a certain type, which shows uncertainties associated with genesis cognition. For instance, suppose that Zn in one deposit is around 5%. Based on Table 3, extracted from Table 2, rough ranges of some parameters in three well-known geneses of sulfide deposits are shown. The genesis might be SEDEX, MVT or VMS.

The aim of the current paper is to find an answer to this question that how it is possible to consider a unique, reliable, and reproducible genesis for a deposit based on the visible evidences. The results of the BDF approach will be presented. Three evidences are considered for the study: Cu, Pb + Zn, and Ag; their rough ranges are abstracted in Table 3.

Table 2. Selected properties of MVT, SEDEX, and Besshi type deposits.

Number and name of district	Type of deposit	Host rock	Alteration	Form	Ore mineral	Gangue mineral	Main metals (ppm)	Minor metals (ppm)	References
1. Tyndrum, Scotland	MVT	Quartzite, Carbonate	-	Strataband	Galena, Sphalerite, ChalcoPyrite	Quartz-Barite	Zn-Pb	-	[32]
2. Blazna-Gustet, Romania	MVT	Carbonate, Dolomite	Metamorphic	Strataband	Galena, Sphalerite, ChalcoPyrite	Calcite, Barite, Quartz, Dolomite	Zn-Pb	Cu-Ag-Ba-Ti	[33]
3. Iberian, Germany	SEDEX	Volcanic-sedimentary	Silicification, sericitation	Strataband	Pyrite, Galena, Sphalerite, ChalcoPyrite	Calcite, Barite, Quartz, Dolomite	Pb-Zn-Cu	Mn-Fe-Mg-Ag	[34]
4. Fankou, China	MVT	Carbonate-Shale	Dolomitization	Strataband	Galena, Sphalerite, Pyrite	Quartz, Calcite, Dolomite	Pb-Zn	Ag-Sb-Se-Te Ag=21-210 -(Cu=76)	[35]
5. Navan, Ireland	SEDEX	Carbonate-Shale-volcanic rocks	Dolomitization	Strataband	Sphalerite, Galena, Pyrite, Marcasite	Calcite, Barite, Dolomite	Zn-Pb>30% -Cu	Mn-Fe-Mg-Ag	[36]
6. Benue Trough, Nigeria	MVT	Shale, Siltstone, limestone	-	Strataband	Galena, Sphalerite, ChalcoPyrite, bornite, Pyrite	Quartz, Calcite, Dolomite, Barite, Fluorite	Pb-Zn	Fe, Mn (Ag=62-140)-(Cu=350)	[37]
7. Broken Hill, Australia	SEDEX	Siltstone-sandstone-	Metamorphic	Strataband, Stratiform	Galena, Sphalerite, Pyrite	Carbonate, Fluorite, Dolomite	Pb-Zn-Ag-Cu	F- Mn- Fe	[25]

		claystone-volcanic rocks							
8. Pyreneez, France	SEDEX	Carbonate-Shale-rhyolite	Dolomitization	Stratiform	Sphalerite, Galena, Pyrite, Marcasite	Calcite, Barite, Quartz	Zn-Pb<10% -Ba	Ni-Co-Ti	[38]
9. Malines, France	MVT	Carbonate-Shale	-	Strataband, Stratiform	Galena, Sphalerite, Pyrite	Quartz, Calcite, Dolomite	Zn-Pb	F-Ba	[39]
10. Zlate Hory, Czechoslovakia	Besshi	Schist, Quartzite, marble	Metamorphic	Strataband, Massive	Sphalerite, Galena, ChalcoPyrite, Pyrite	Quartz, cCalcite, Dolomite	Zn-Pb-Cu	Au-Bi-Ag	[28]
11. Tharsis mine, Spain	VMS	Carbonaceous black slate-volcanic group	Metamorphic	Stratiform	Pyrite, Sphalerite, Galena, ChalcoPyrite, ArsenoPyrite	Calcite, Dolomite, Quartz	Pb-Zn< 2.6% (Cu=8000)	Bi-Te	[40]
12. Bleikvassli, Norway	SEDEX	Amphibolites-schist, gneiss, marble	Metamorphic	Stratiform-Lenses	Pyrite, Sphalerite, Galena, ChalcoPyrite, ArsenoPyrite	Quartz	Zn-Pb<12% (Cu=4000)	Ag-Sb	[41]
13. Malmani, South Africa	MVT	Carbonate-Dolomite	-	Stratiform, Strataband	Sphalerite, Galena, ChalcoPyrite, Pyrite	Calcite, Dolomite	Pb-Zn<4.3% -F	Fe-Mn-(Ag=70-300)	[42]
14. Yindongzi, China	SEDEX	Meta Siltstone, Shale, limestone	Argillic-silicic-albitization	Strataband	Galena, Sphalerite, ChalcoPyrite, ArsenoPyrite, Pyrrhotite	Carbonate, Barite, Quartz	Pb-Zn<11% - Cu	Fe- Na – Mg-(Ag=54-100)	[43]
15. Ponferrada, Spain	MVT	Carbonate-dolostone-Shale	-	Strataband	Pyrite, Sphalerite, Galena	Calcite, Quartz	Zn – Pb<17.6%	Cu-(Ag=48)	[44]
16. Pucara Basin, Peru	MVT	Carbonate-Dolomite	-	Strataband	Sphalerite, Galena, Marcasite, Pyrite	Calcite, Dolomite	Pb-Zn<10%	F-Ba-(Ag=31)	[45]
17.Lengenbach, Switzerland	SEDEX	Dolostone – green schist-amphibolites	Silicic	Strataband, Stratiform	Galena, Sphalerite, Pyrite	Carbonate, Barite, Quartz	Pb-Zn-Cu	As-Tl-Ba-(Ag=10-426)	[46]
18. Santa Lucia, Cuba	SEDEX	Dolostone-Shale-limestone-schist	-	Stratiform	Galena, Sphalerite, Pyrite, ChalcoPyrite	Carbonate, Barite, Quartz	Zn- Pb<6% (Cu=1600)	Ba-(Ag=3-120)	[47]
19. Yenefrito, Spain	SEDEX	Siltstones, marls and limestone porphyritic sills	Propylitized	Stratiform, Lenticular	Sphalerite, Arsenopyrite, Galena, Pyrite, Chalcopyrite	Quartz, Calcite	Zn - Pb - Cu		[48]
20. Damaran Lufilian, Central Africa	SEDEX	MetaCarbonates, Dolomite	Metamorphism	Epigenetic, Massive, Pipe-Like	Galena, tennantite, Sphalerite, Chalcocite, bornite, and enargite	Quartz, Calcite	Pb-Zn<35.9% -Cu	Ge, Cd, As, Sb, Ag, Au	[49]
21. Kuh-e-Surmeh, Iran	MVT	Carbonate	-	Strataband	Sphalerite and Galena,Pyrite, ChalcoPyrite, Covellite, Chalcocite, Marcasite	Dolomite, Barite, gypsum	Zn-Pb<17.5%		[50]
22. Angouran, Iran	MVT? SEDEX? Massive Sulfide?	Amphibolites, gneiss, marble	Metamorphism	Strataband, Stratiform	Sphalerite, Galena,Pyrite	Quartz, Dolomite, anhydrite, Calcite	Zn-Pb<29% - (Ag=210)	Co, Ni, (Cu=250)	[51]
23. George Fisher, Australia	SEDEX	Shale, Siltstone, Carbonate, tuff	Silica Dolomite Alteration	Strataband, Lenses	Sphalerite, Galena, Pyrrhotite, Pyrite	Calcite, Dolomite, Quartz, Fluorite	Zn-Pb<16.5%-(Cu=5000)	Ag=93-150	[52]
24. Nanisivik, Canada	MVT	Dolomitic Mudstone	-	Strataband - Lenses	Sphalerite, Galena, Pyrite, Marcasite	Dolomite, Calcite	Pb- Zn<10%	(Cu=46)-(Ag=35)	[24]
25. Mount Isa, Australia	SEDEX	Dolomitic Shale, Siltstones, and Mudstones	Silica-Dolomite	Strata-Bound	Pyrite, Sphalerite and Galena,Barite	Calcite, Dolomite, Quartz, Fluorite	Zn-Pb<13% - (Cu=3000)	Ag=150	[53]
26. Upton, Canada	MVT	Limestone, Clastic Rocks	-	Strataband	Sphalerite, Pyrite, Galena	Calcite, Barite	Zn-Pb<2.1% - Ba	(Ag= 13.5)-(Cu=130)-Cd	[54]
27. Red Gog, Northern Alaska	SEDEX	Chert, Carbonate, Mudstone and Shale	-	Stratiform – Lens	Sphalerite, Galena, Pyrite, Marcasite ChalcoPyrite	Barite, Calcite	Zn-Pb<21% - (Cu=1000)	(Ag=230)-Au	[55]
28. McArthur, Australia	SEDEX	Dolomitic Siltstone	Silica-Dolomite	Stratiform	Pyrite, Sphalerite, ChalcoPyrite, Galena, ArsenoPyrite	Quartz	Zn-Pb<19% - Cu	(Ag=60)-Tl-Fe	[56]
29. Maestrat basin, Spain	MVT	Limestones	-	Strataband	Sphalerite, Galena, Pyrite, Marcasite	Dolomite	Zn-Pb<8%	Cu	[57]

30. Basque-Cantabrian, Spain	MVT	Limestones	Dolomitized	Strataband	Sphalerite and Galena, Marcasite, Pyrite	Barite, Calcite	Zn-Pb<9.4%	(Ag=5)-Au -(Cu=50)	[58]
31. Illinois-Kentucky, USA	MVT	Carbonate, Clastic Units	-	Strataband	Sphalerite, Galena, Pyrite	Dolomite, Fluorite	Zn-Pb	Cu-Ag	[58]
32.Corrdileran, Canada	MVT	Limestones	Dolomitized	Strataband	Sphalerite, Galena, Pyrite	Quartz, Calcite, Dolomite	Zn-Pb<7.1%	-	[59]
33. McArthur River (HYC), Australia	SEDEX	Limestone-Shale	Stratiform-lenses	Sphalerite and Galena, Pyrite	Barite, Calcite, Dolomite	Barite, Calcite, Dolomite	Zn-Pb-(Cu=2000)	(Ag=41)-Au	[60]
34. Lengshuikeng, China	SEDEX	Volcano sedimentary rocks	-	Strataband	Sphalerite, Galena, Pyrite	Calcite, dolomite	Zn-Pb<4.6%	(Ag=204)	[61]
35. Wusihe, China	MVT	Carbonate	-	Stratiform	Pyrite, galena, Sphalerite	Calcite, dolomite	Zn-Pb<11%	-	[62]
36. Chahmir, Iran	SEDEX	Volcano sedimentary rocks	Silicification, carbonitization	Strataband	Pyrite, galena, Sphalerite	Calcite, dolomite, quartz	Zn-Pb<8%	-	[63]
37. Howards Pass, Yukon	SEDEX	Volcano sedimentary rocks	-	Strataband	Pyrite, galena, Sphalerite	Calcite, dolomite	Zn-Pb<6%	-	[64]

3.1. Case Study

The Angouran Zn-Pb-Ag deposit is located in the Western Zanjan Province, NW Iran, about 450 km NW Tehran (Figure 2; compiled from [65, 66]). The Angouran deposit is a world class and the largest zinc deposit in Iran. The ore deposit resources are about 14.6 MT with 22.6% zinc, 4.6% lead, and 110 ppm silver [67]. The Angouran deposit is located within the Sanandaj-Sirjan metamorphic belt, and the host rocks are marble, micaschist, amphibolites, and gneiss of Cambrian. Many have worked on the genesis of **the Angouran deposit** since 1968 with numerous developed models, to be named a few Proterozoic volcanogenic massive sulfide (VMS)-type mineralization [68], sedimentary-exhalative (SEDEX) process during the Mesozoic [67], and the Mississippi Valley type (MVT) deposit [51]. Therefore, it seems that the genesis for this deposit is rather conflicting between reports appearing in the early 2000s. Something we believe that is required to be rectified is through implementing a proper methodology that minimizes the uncertainty during identification of a deposit.

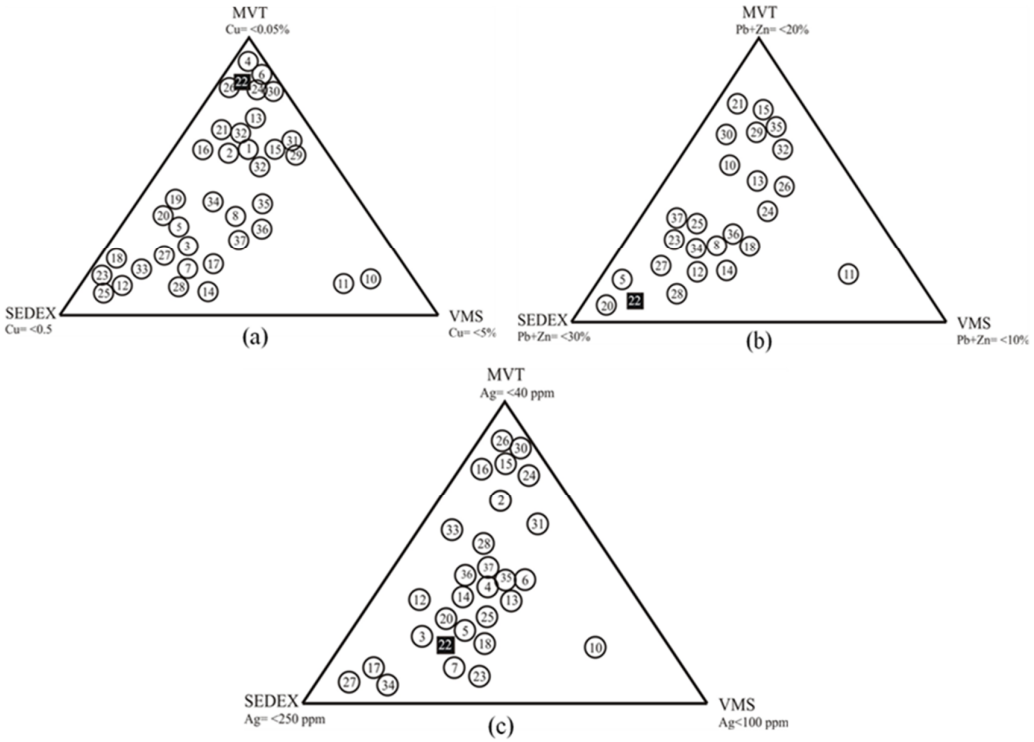

Figure 1. Three well-known geneses of Pb-Zn type deposits. Concentrations of characteristic elements in MVT, SEDEX, and VMS are displayed. Numbers correspond to the numbers of deposits in Table 2, first column. Square is Angouran's deposit. Location of the circles and square are based on the average analysis of a) Cu, b) Zn + Pb, and c) Ag, reported for each mine.

Table 3. The rough ranges of Cu, Pb, Zn, Pb + Zn, and Ag extracted from Table 2, for three well-known geneses of sulfide deposits, *i.e.* Mississippi Valley (MV), Massive Sulfide (MS), and SEDEX (S).

	SEDEX	MVT	VMS
Cu (%)	0.05 - 0.5	Up to 0.05	0.5 - 5
Pb (%)	0.1 - 15	1 - 6	0.01 - 0.1
Zn (%)	1 - 16	1 - 16	0.1 - 6
Pb+Zn (%)	1 - 31	2 - 22	0.1 - 6
Ag (ppm)	1 - 250	0.1 - 40	1 - 100

4. Schematic dataset

Properties (3), Cu, Pb+Zn, and Ag, are listed in Table 3 for analysis of the Angouran's genesis. The data was analyzed and compared for the case of 2, Cu and Pb + Zn (Table 4), and 3 properties (Table 5), as indicated. Furthermore, prospecting and the general exploration stages were considered for analysis via BDF with the assumptions of 1) availability of the information for only 3 properties, Cu, Pb + Zn, and Ag 2) considering only 3 genesis types, Mississippi Valley, Massive Sulfide or SEDEX Sulfide, according to Figure 1. Results of analysis of the prospecting stage were fused together using Equations 2, 3, 4, and 5, and these results were reported in the last rows of Tables 4 and 5. A priori knowledge for the three common deposit types was considered the same and equal to:

$$P(MV) = P(MS) = P(S) = \frac{1}{3}$$

The comparison of the Angouran deposit belonging probability with three geneses based on the previous datasets (first row in Table 4) and the results of data fusion (when Cu and Pb + Zn are available) (third row in Table 5) show that they have changed as follow:

- Mississippi Valley Type: from 50% (average of two properties) to 70.5%,
- Massive Sulfide: from 35% (average of two properties) to 26.5%, and
- SEDEX Sulfide: from 15% (average of two properties) to 3.0%.

This shows that data fusion has amplified the probability of Mississippi Valley Type for Angouran, while it has been attenuated for the two other types.

Comparisons between Tables 4 and 5 are interesting. The probabilities of third property (Ag, in this case) were considered to be equal to average of properties 1 and 2 (Cu and Pb + Zn, in this case). Therefore, it is anticipated that the results of fusion of three properties (third row, Table 5) should be similar to the results of fusion of two properties (third row, Table 4). However, the results were completely different (Data fusion when Cu, Pb + Zn, and Ag are available):

- Mississippi Valley Type: from 50% (average of two properties) to 81.7%,
- Massive Sulfide: from 35% (average of two properties) to 17.7%, and
- SEDEX Sulfide: from 15% (average of two properties) to 0.6%.

It should be emphasized that in both case studies (2 or 3 properties), based on the situations, the average belonging probability was considered to be the same (first row in Tables 4 and 5). The comparison shows that BDF amplifies discrimination between geneses when more properties are used. Of a great interest is the considerable reduction of uncertainties (smaller than 30%) in both cases with 2 and 3 properties. For the sake of clarification, the average belonging value improved from 50% to 70.5% for 2 properties (Table 4) and 81.7% for 3 properties (Table 5).

5. Result of data fusion

In this part, the results of the previous datasets and current datasets (prospecting and general exploration in Tables 4 and 5) are fused. The following equation is used for fusion of the results for two properties (in different exploration stages) in the Mississippi Valley type:

$$P(MV|Y_1^1 Y_1^2 Y_0^1 Y_0^2) = \frac{P(MV|Y_0^1 Y_0^2)P(MV|Y_1^1)P(MV|Y_1^2)}{P(MV|Y_0^1)P(MV|Y_0^2)} \times \frac{1}{Normalization\ Factor} \quad (8)$$

where all the terms were calculated in Tables 4 and 5. It should be reiterated that the summation of probabilities have to be equal to one, which is the role of the normalization factor. The equation for the data fusion calculation result in the case of three

properties in the Mississippi Valley type is abstracted as follows:

$$P(MV|Y_1^1Y_1^2Y_1^3Y_0^1Y_0^2Y_0^3) = \frac{P(MV|Y_0^1Y_0^2Y_0^3)P(MV|Y_1^1)P(MV|Y_1^2)P(MV|Y_1^3)}{P(MV|Y_0^1)P(MV|Y_0^2)P(MV|Y_0^3)} \times Normalization\ Factor \quad (9)$$

All terms were defined in Tables 4 and 5.

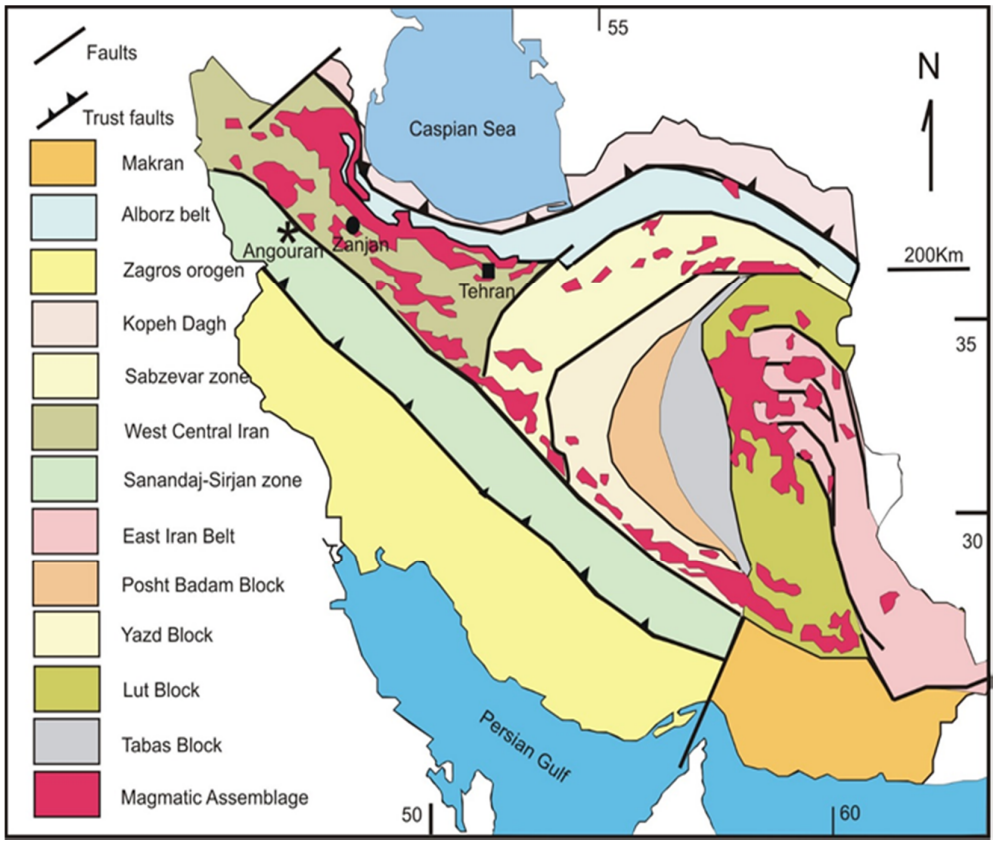

(a)

(b)

Figure 2. a) Simplified tectonic map of Iran (compiled from [65 – 66]). The star shows the location of the Angouran deposit. b) A panorama photo of Angouran lead and zinc mine.

Table 4. Fuzzy values for a schematic study on Angouran's deposit considering all 3 geneses (Figures 1) based on the results of analysis of two sensors: Cu and Pb + Zn.

Dataset	First Sensor (Cu)	Second Sensor (Pb+Zn)
Previous Dataset (Prospecting)	$P(MV\|Y_0^1) = 0.4$ $P(S\|Y_0^1) = 0.4$ $P(MS\|Y_0^1) = 0.2$	$P(MV\|Y_0^2) = 0.6$ $P(S\|Y_0^2) = 0.3$ $P(MS\|Y_0^2) = 0.1$
Current Dataset (General Exploration)	$P(MV\|Y_1^1) = 0.7$ $P(S\|Y_1^1) = 0.17$ $P(MS\|Y_1^1) = 0.13$	$P(MV\|Y_1^2) = 0.8$ $P(S\|Y_1^2) = 0.15$ $P(MS\|Y_1^2) = 0.05$
Fusion of Previous Dataset (Prospecting stage)	$O(MV\|Y_0^1Y_0^2) = \frac{\frac{1}{3}}{\frac{2}{3}} \cdot \frac{0.6}{0.4} \cdot \frac{0.4}{0.6} = 0.5$ $P_{before\ normalization}(MV\|Y_0^1Y_0^2) = \frac{0.5}{1 + 0.5} = 0.333$ $P(MV\|Y_0^1Y_0^2) = \frac{0.333}{0.333 + 0.125 + 0.014} = 0.706 = 70.5\%$	
	$O(S\|Y_0^1Y_0^2) = \frac{\frac{1}{3}}{\frac{2}{3}} \cdot \frac{0.3}{0.7} \cdot \frac{0.4}{0.6} = 0.143$ $P_{before\ normalization}(S\|Y_0^1Y_0^2) = \frac{0.143}{1 + 0.143} = 0.125$ $P(S\|Y_0^1Y_0^2) = \frac{0.125}{0.333 + 0.125 + 0.014} = 0.265 = 26.5\%$	
	$O(MS\|Y_0^1Y_0^2) = \frac{\frac{1}{3}}{\frac{2}{3}} \cdot \frac{0.1}{0.9} \cdot \frac{0.2}{0.8} = 0.014$ $P_{before\ normalization}(MS\|Y_0^1Y_0^2) = \frac{0.014}{1 + 0.014} = 0.014$ $P(MS\|Y_0^1Y_0^2) = \frac{0.014}{0.333 + 0.125 + 0.014} = 0.030 = 3.0\%$	

MV, MS, and S stand for Mississippi Valley, Massive Sulfide and SEDEX types, respectively.

The results of applying BDF to all data are summarized in Tables 6 (in the case of two properties, Cu and Pb + Zn) and 7 (in the case of three properties, Cu, Pb + Zn, and Ag). Of a great interest is the fact that the application of data fusion improved the probability of the belonging from an average of 75% to nearly 100% (99.6%, 99.36% for 2 and 3 properties, respectively), which means less uncertainties in identification of the deposit (Tables 6 and 7).

Results of the Angouran deposit belonging probability to three geneses are based on fusion of prospecting and general exploration dataset (first and second rows in Tables 6 and 7), in the cases that two or three properties generated interesting results. BDF concluded that with a probability more than 99%, the Angouran's type is Mississippi Valley, with an uncertainty in decision-making close to zero. As a result, in the detailed exploration procedure, the patterns of the Mississippi Valley type must be utilized.

When two-stage datasets are available, numbers of properties are not so important, and there are no significant differences between the final results. In the case study, the Angouran's belonging probability to the Mississippi Valley type were equal to 99.6 % and 99.36 % for two and three properties, respectively.

6. How proposed method could be applied to exploration programs

Identification of the ore deposit genesis, which is one of the main duties of economic geologists, is an important step in exploration, surveying, sampling, and reserve modeling. There are also usually evidences for known genesis (e.g. Tables 1 and 2); the similarity between those evidences and field observations helps to identify ore deposit genesis. The scientists have often different ideas about the genesis of a certain deposit (more example is in case 3.1). This uncertainty makes the exploration activities rather costly with disparity in classification outcome. The introduced procedure helps to integrate the evidences or even different hypotheses about the genesis of ore deposits in order to decrease the uncertainty associated with, which leads to utilize the suggested exploratory pattern for the identified genesis type.

Table 5. Fuzzy belonging values of schematic study on Angouran's deposit considering all 3 geneses (Figures 1) based on the results of analysis of three sensors: Cu, Pb+Zn, and Ag.

Dataset	First Sensor (Cu)	Second Sensor (Pb+Zn)	Third Sensor (Ag)
Previous Dataset (Prospecting)	$P(MV\|Y_0^1) = 0.40$ $P(S\|Y_0^1) = 0.40$ $P(MS\|Y_0^1) = 0.20$	$P(MV\|Y_0^2) = 0.60$ $P(S\|Y_0^2) = 0.30$ $P(MS\|Y_0^2) = 0.10$	$P(MV\|Y_0^3) = 0.50$ $P(S\|Y_0^3) = 0.35$ $P(MS\|Y_0^3) = 0.15$
Current Dataset (General Exploration)	$P(MV\|Y_1^1) = 0.70$ $P(S\|Y_1^1) = 0.17$ $P(MS\|Y_1^1) = 0.13$	$P(MV\|Y_1^2) = 0.80$ $P(S\|Y_1^2) = 0.15$ $P(MS\|Y_1^2) = 0.05$	$P(MV\|Y_1^3) = 0.75$ $P(S\|Y_1^3) = 0.16$ $P(MS\|Y_1^3) = 0.09$
Fusion of Previous Dataset (Prospecting stage)	$O(MV\|Y_0^1Y_0^2Y_0^3) = \frac{\frac{1}{3}}{\frac{2}{3}} \cdot \frac{0.6}{0.4} \cdot \frac{0.4}{0.6} \cdot \frac{0.5}{0.5} = 0.5$ $P_{before\ normalization}(MV\|Y_0^1Y_0^2Y_0^3) = \frac{0.5}{1 + 0.5} = 0.333$ $P(MV\|Y_0^1Y_0^2Y_0^3) = \frac{0.333}{0.333 + 0.072 + 0.0025} = 0.817 = 81.7\%$		
	$O(S\|Y_0^1Y_0^2Y_0^3) = \frac{\frac{1}{3}}{\frac{2}{3}} \cdot \frac{0.4}{0.6} \cdot \frac{0.3}{0.7} \cdot \frac{0.35}{0.65} = 0.077$ $P_{before\ normalization}(S\|Y_0^1Y_0^2Y_0^3) = \frac{0.077}{1 + 0.077} = 0.072$ $P(S\|Y_0^1Y_0^2Y_0^3) = \frac{0.072}{0.333 + 0.072 + 0.0025} = 0.177 = 17.7\%$		
	$O(MS\|Y_0^1Y_0^2Y_0^3) = \frac{\frac{1}{3}}{\frac{2}{3}} \cdot \frac{0.2}{0.8} \cdot \frac{0.1}{0.9} \cdot \frac{0.15}{0.85} = 0.0025$ $P_{before\ normalization}(MS\|Y_0^1Y_0^2Y_0^3) = \frac{0.0025}{1 + 0.0025} = 0.0025$ $P(MS\|Y_0^1Y_0^2Y_0^3) = \frac{0.0025}{0.333 + 0.072 + 0.0025} = 0.006 = 0.6\%$		

MV, MS, and S stand for Mississippi Valley, Massive Sulfide, and SEDEX types, respectively.

Table 6. Summarized results of data fusion-based genesis recognition of the studied schematic deposit using the dataset for two sensors: Cu and Pb + Zn.

Genesis Type	Data Fusion of Previous Dataset (Prospecting Stage)	Current Dataset (General Exploration Stage)		Final Data Fusion
		First Sensor (Cu)	Second Sensor (Pb + Zn)	
Mississippi Valley	70.5%	70%	80%	$P_{before\ normalization}(MV\|Y_1^1Y_1^2Y_0^1Y_0^2) = \frac{0.705 \times 0.80 \times 0.70}{0.40 \times 0.60} = 16.45$ $P(MV\|Y_1^1Y_1^2Y_0^1Y_0^2) = \frac{16.45}{16.45 + 0.0563 + 0.00975} = 0.996 = 99.6\%$
SEDEX	26.5%	17%	15%	$P_{before\ normalization}(S\|Y_1^1Y_1^2Y_0^1Y_0^2) = \frac{0.265 \times 0.17 \times 0.15}{0.40 \times 0.30} = 0.0563$ $P(S\|Y_1^1Y_1^2Y_0^1Y_0^2) = \frac{0.0563}{16.45 + 0.0563 + 0.00975} = 0.0034 = 0.34\%$
Massive Sulfide	3%	13%	5%	$P_{before\ normalization}(MS\|Y_1^1Y_1^2Y_0^1Y_0^2) = \frac{0.03 \times 0.13 \times 0.05}{0.20 \times 0.10} = 0.00975$ $P(MS\|Y_1^1Y_1^2Y_0^1Y_0^2) = \frac{0.00975}{16.45 + 0.0563 + 0.00975} = 0.0006 = 0.06\%$

Table 7. Summarized results of data fusion based genesis recognition of the studied schematic deposit using the dataset for three sensors: *i.e.* Cu, Pb + Zn, and Ag.

Genesis Type	Data Fusion of Previous Dataset (Prospecting Stage)	Current Dataset (General Exploration Stage)			Final Data Fusion
		First Sensor (Cu)	Second Sensor (Pb + Zn)	Third Sensor (Ag)	
Mississippi Valley	81.7%	70%	80%	75%	$P_{before\ normalization}(MV\|Y_1^1Y_1^2Y_1^3Y_0^1Y_0^2Y_0^3) = \frac{0.817 \times 0.70 \times 0.80 \times 0.75}{0.40 \times 0.60 \times 0.50} = 2.8595$ $P(MV\|Y_1^1Y_1^2Y_1^3Y_0^1Y_0^2Y_0^3) = \frac{2.8595}{2.8595 + 0.0172 + 0.00975} = 0.9936 = 99.36\%$
SEDEX	17.7%	17%	15%	16%	$P_{before\ normalization}(S\|Y_1^1Y_1^2Y_1^3Y_0^1Y_0^2Y_0^3) = \frac{0.177 \times 0.17 \times 0.15 \times 0.16}{0.40 \times 0.30 \times 0.35} = 0.0172$ $P(S\|Y_1^1Y_1^2Y_1^3Y_0^1Y_0^2Y_0^3) = \frac{0.0172}{2.8595 + 0.0172 + 0.00975} = 0.006 = 0.6\%$
Massive Sulfide	0.6%	13%	5%	9%	$P_{before\ normalization}(MS\|Y_1^1Y_1^2Y_1^3Y_0^1Y_0^2Y_0^3) = \frac{0.006 \times 0.13 \times 0.05 \times 0.09}{0.20 \times 0.10 \times 0.15} = 0.00117$ $P(MS\|Y_1^1Y_1^2Y_1^3Y_0^1Y_0^2Y_0^3) = \frac{0.00117}{2.8595 + 0.0172 + 0.00117} = 0.0004 = 0.04\%$

For example, as implied in Tables 6 and 7, data fusion has been concluded that with a probability more than 99%, Angouran's type is Mississippi Valley. Therefore, it means that certainly, genesis is Mississippi Valley type and uncertainty in decision-making nears zero. As a result, in the detailed exploration procedure, the patterns of Mississippi Valley type must be utilized.

On the other hand, the introduced procedure might help to recognize the belts of lead and zinc with the geneses MVT, SEDEX, and Massive Sulfide. This will lead to useful prospecting patterns. Similar procedure could be developed for Porphyry-type Copper deposits, Manto-type Copper deposits, Iron ore deposits, etc.

7. Conclusions

Identification of the ore deposit genesis, which is important in optimization of exploration activities, is a challenging decision in economic geology. There are usually evidences for known genesis; similarity between those evidences and field observations help to identify ore deposit genesis. The scientists have often different ideas about genesis of a certain deposit. This uncertainty makes the exploration activities rather costly with disparity in classification outcome.

In the current paper, Bayesian Data Fusion (BDF) was introduced and applied to achieve a unique genesis type for a deposit based on various stages of exploration datasets. A schematic problem was designed to show how BDF works and how it helps to discriminate between various possible geneses. Angouran's challenge matched with the designed problem in order to make a well-defined issue. The results obtained show that data fusion amplifies the deposit belonging probability to a genesis and attenuation of other types. Therefore, it helps to decrease the uncertainty associated with knowledge of scientists' judgments, and further helped enormously in identification of a deposit.

References

[1]. Mosier, D.L. and Bliss, J.D. (1991). Introduction and overview of mineral deposit modeling, USGS Publication Warehouse, 5.

[2]. Guilbert, J.M. and Park, Jr. C.F. (2007). The Geology of Ore Deposits, Waveland Press.

[3]. Carranza, E.J.M. (2009). Handbook of Exploration and Environmental Geochemistry, Chapter 7: Knowledge-Driven Modeling of Mineral Prospectivity. pp. 189-247. and Chapter 8: Data-Driven Modeling of Mineral Prospectivity. 11: 249-310.

[4]. Evans, A.M. (2009). Ore Geology and Industrial Minerals, An Introduction, Third Edition, WILEY-BLACKWELL.

[5]. Tosovic, R. (2016). General review of the genetic and geological – economic modeling of the mineral deposits of Serbia. International Journal of Research Granthaalayah. 4 (6): 38-45.

[6]. Callahan, W.H. and Momurry, H.V. (1967). Geophysical exploration of Mississippi valley-Appalachian type strata-bound zinc-lead deposits. Geology Survey of Canada Report. 26: 350-360

[7]. De Geoffroy, J. and Wignall, T.K. (1973). Design of a statistical data processing system to assist regional exploration planning. Canadian Mining Journal. 94 (11). 30-35 and 94 (12): 35-36.

[8]. Einaudi, M.T. and Burt, D.M. (1982). Introduction, Terminology. Classification, and Composition of Skarn Deposits: Economic Geology. 77: 745-754.

[9]. Cox, D.P. and Singer, D.A. (1991). Classification of Deposit Models, In Orris, U.S. Geological Survey Bulletin. Washington.

[10]. Orris, G.J. and Bliss, J.D. (1992). Some Industrial Mineral Deposit Models; Grade Tonnage Deposit Models. US Geological Survey. Open – File Report 91 – 11B.

[11]. Singer, D.A., and Mosier, D.L. (1993). Mineral deposit grade-tonnage models: U. S. Geological Survey Open –File Report. 93-623. 100.

[12]. Wellmer, F.W. (1998). Statistical Evaluation in Exploration of Mineral Deposits, Springer New York.

[13]. Yang, X.Z., Ishihara, S. and Zhao, D.H. (2006). Genesis of the Jinchuan PGE deposit, China: evidence from fluid inclusions, mineralogy and geochemistry of precious elements**.** Mineralogy and Petrology**.** 86: 109–128.

[14]. Hitzman, M.W., Reynolds, N.A. and Sangster, D.F. (2003). Allen C.R. and Carman C.E., Classification, Genesis, and Exploration Guides for Nonsulfide Zinc Deposits, Economic Geology. 98 (4): 685-714.

[15]. Sarparandeh, M. and Hezarkhani, A. (2016). Application of Self-Organizing Map for Exploring of REEs' Deposition. Open Journal of Geology. 6: 571–582.

[16]. Rodkin, M.V. and Shatakhtsyan, A.R. (2015). Study of ore deposits by the dynamic systems investigation methods: 2. clustering of ore deposits and interpretation of the results. 51 (3): 428–436.

[17]. Sarparandeh, M. and Hezarkhani, A. (2017). Application of unsupervised pattern recognition approaches for exploration of rare earth elements in Se-Chahun iron ore, central Iran. Geoscientific Instrumentation Methods and Data Systems. 6: 537–546.

[18]. Gros, X.E. (1997). NDT Data Fusion, John Wiley & Sons, New York.

[19]. Hall, D.L. and Llinas, J. (2001). Handbook of multisensory data fusion. CRC Press LLC. Boca Raton.

[20]. Tahani, H. and Keller, J.M. (1990). Information fusion in computer vision using the fuzzy integral systems. Man and Cybernetics. 20 (3): 733-741.

[21]. Russo, F. and Ramponi, G. (1994). Fuzzy methods for multisensory data fusion, IEEE Transactions on Instrumentation and Measurement. 43 (2): 288-294.

[22]. Bleiholder, J. and Naumann, F. (2008). Data Fusion. ACM Computing Surveys. 41 (1): 1-41.

[23]. Tokhmechi, B., Lotfi, M., Seifi, H. and Hosseini M.S. (2017). Data Fusion, a new approach for decision making in geology, mining and petroleum engineering. Amirkabir University of Technology (Tehran Polytechnic) Publications. ISBN: 978-964-463-656-1, 808.

[24]. Sherlock, R.L., Lee, J.K.W. and Cousens, B.L. (2004). Geology and geochronologic constraints on the timing of mineralization at the Nanisivik zinc-lead Mississippi valley type deposit northern Baffin island, Nunavut, Canada, Economic Geology. 99: 279-293.

[25]. Plimer, I.R. (1985). Broken Hill Pb-Zn-Ag deposit-a product of mantle metasomatism, Mineralium Deposita. 20: 147-153.

[26]. Patocka, F. and Vrba, J. (1989). The comparison of strata-bound massive sulfide deposits using the fuzzy-linguistic diagnosis of the Zlate Hory deposits, Czechoslovakia, as an example, Mineralium Deposita. 24: 192-104.

[27]. Challa, S. and Koks, D. (2004). Bayesian and Dempster-Shafer fusion. Sadhana. 29 (2): 145-174.

[28]. Jensen, M.L. and Bateman, A.M. (1981). Economic Mineral Deposits, 3rd edition, New York. John Wiley & Sons.

[29]. Edwards, R. and Atkinson, K. (1986). Ore Deposit Geology, Chapman and Hall Pub.

[30]. McKelvey, G.E. and Bliss, J.D. (1991). Application of grade and tonnage models to the development of strategies for mineral deposit exploration [abs.], in Good E.E., Slack L.F. and Koutra P.K., eds., USGS research on mineral resources; US Geological Survey Circular. 1062: 53-54.

[31]. McCammon, R.B. (1992). Numerical Mineral Deposit Models, in Developments in Mineral Deposits Modeling, James D. Bliss Editor. US Geological Survey. Bulletin No. 2004.

[32]. Pattrick, R.A.D., Coleman, M.L. and Russell, M.J. (1983). Sulphur isotopic investigation of vein lead-zinc mineralization at Tyndrum, Scotland, Mineralium Deposita. 18: 477-485.

[33]. Udubasa, G., Nedelcu, L., Andar, A. and Andar, P. (1983). Strataband lead- zinc Pyrite ore deposits in upper Precambrian Carbonate rocks, Rodana Mountains, Romania, Mineralium Deposita. 18: 519-828.

[34]. Moller, P. Dieterle, M.A. Dulski, P. Germann, K., Schneider, H.J. and Schutz, W. (1983). Geochemical proximity indicators of massive sulphide mineralization in the Iberian Pyrite Belt and the east Ponic Metallotect, Mineralium Deposita. 18: 387-398.

[35]. Xuexin, A. (1984). Minor elements and ore genesis of the fankou lead-zinc deposit, Cina, Mineralium Deposita. 19: 95-104.

[36]. Kucha, H. and Wieczorek, A. (1984). Sulfide-Carbonate relationships in the Navan (Tara) Zn-Pb deposit, Ireland, Mineralium Deposita. 19: 208-216.

[37]. Olade, M.A. and Morton, R.D. (1985). Origin of lead-zinc mineralization in the southern Benue Trough, Nigeria-Fluid inclusion and trace element studies, Mineralium Deposita. 20: 76-80.

[38]. Pouit, G. and Bois, J.P. (1986). Arrens Zn (Pb), Ba Devonian deposit, Pyrenees, France. An exhalative-sedimentary-type deposit similar to Meggen, Mineralium Deposita. 21: 181-189.

[39]. Charef, A. and Sheppard, S.M.F. (1988). The Malines Cambrian Carbonate-Shale-hosted Pb-Zn deposit, France. Thermometric and isotopic (H, O) evidence for pulsating hydrothermal mineralization, Mineralium Deposita. 23: 86-95.

[40]. Kase, K., Yamamoto, M., Nakamura, T. and Mitsuno, C. (1990). Ore mineralogy and sulfur isotope study of the massive sulfide deposit of Filon Norte, Tharsis mine, Spain, Mineralium Deposita. 25: 289-296.

[41]. Skauli, H., Boyce, A.J. and Fallick, A.E. (1992). A sulphur isotope study of the Beikvassli Zn-Pb-Cu deposit, Nordland, northern Norway, Mineralium Deposita. 27: 284-292.

[42]. Martini, J.E.J., Eriksson, P.G. and Snyman, C.P. (1995). The early Proterozoic Mississippi valley type Pb-Zn-F deposits of the Campbellrand and Malmani Subgroup, South Africa, Mineralium Deposita. 30: 135-145.

[43]. Jiang, S.y., Palmer, M.R., Li, Y.H. and Xue, C.J. (1995). Chemical compositions of tourmaline in the Yindongzi-Tongmugou Pb-Zn deposits, Qinling, China. Implications for hydrothermal ore-forming processes, Mineralium Deposita. 30: 225-234.

[44]. Tornos, F., Ribera, F., Shepherd, T.J. and Spiro, B. (1996). The geological and metallogenic setting of strataband Carbonate-hosted Zn-Pb mineralization in the west Asutrian Leonese zone, NW Spain, Mineralium Deposita. 31: 27-40.

[45]. Mortz, R., Fontbote, L., Spangenberg, J., Rosas, S., Sharp, Z. and Fontignie, D. (1996). Sr, C and O isotope systematic in the Pucara Basin, central Peru. Comparison between Mississippi valley type deposits and barren areas, Mineralium Deposita. 31: 147-162.

[46]. Hofmann, B.A. and Knill, M.D. (1996). Geochemistry and genesis of the Lengenbach Pb-Zn-As-Tl-Ba-mineralization, Binn valley, Switzerland, Mineralium Deposita. 31: 319-339.

[47]. Valdes-Nodarse, E.L. (1998). Pb-Zn "SEDEX" deposits and their copper stockwork roots, western Cuba, Mineralium Deposita. 33: 560-567.

[48]. Subias, I., Fanlo, I., Yuste, A. and Fernandez-Nieto, C. (1999). The Yenefrito Pb-Zn mine (Spanish central Pyrenees) and example of superimposed metallogenetic events, Mineralium Deposita. 34: 220-223.

[49]. Kamona, A.F., Leveque, J., Friedrich, G. and Haack, U. (1999). Lead isotopes of the Carbonate-hosted Kabwe, Tsumeb, and Kipushi Pb-Zn-Cu sulphide deposits in relation to Pan Africa orogenesis in the Damaran-Lufilian fold Belt of central Africa, Mineralium Deposita. 34: 273-283.

[50]. Liaghat, S., Morre, F. and Jami, M. (2000). The Kuh-e-Surmeh mineralization, a Carbonate Zn-Pb deposit in the simply folded belt of the Zagros Mountains, SW Iran, Mineralium Deposita. 35: 72-78.

[51]. Gilg, H.A., Boni, M., Balassone, G., Allen, C.R., Banks, D. and Moore, F. (2006). Marble-hosted sulfide ores in the Angouran Zn-(Pb-Ag) deposit, NW Iran: interaction of sedimentary brines with a metamorphic core complex, Mineralium Deposita. 41: 1-16.

[52]. Chapman, L.H. (2004). Geology and mineralization styles of the George Fisher Zn-Pb-Ag deposit, Mount Isa, Australia, Economic Geology. 99: 233-255.

[53]. Davis, T.P. (2004). Mine scale structural controls on the mount Isa Zn-Pb-Ag and Cu orebodies, Economic Geology. 99: 543-559.

[54]. Pardis S., Chi, G. and Lavoie, D. (2004). Fluid inclusion and isotope evidence for the origin of the Upton Ba-Zn-Pb deposit, Quebec Appalachians, Canada, Economic Geology. 99: 807-817.

[55]. Kelley, K.D. and Jennings, S. (2004). A special issue devoted to Barite and Zn-Pb-Ag deposits in the Red Dog district, western Brooks Range, northern Alaska, Economic Geology. 99: 1267-1280.

[56]. Ireland, T., large, R.R., Mcgoldrich, P. and Blake, M. (2004). Spatial distribution pattern of sulfur isotopes, nodular Carbonate, and ore textures in the McArthur River (HYC) Zn-Pb-Ag deposit, northern Territory, Australia, Economic Geology. 99: 1687-1709.

[57]. Grandia, F., Dardellach, E., Canalas, A. and Banks, D.A. (2003). Geochemistry of the fluid related to epigenetic Carbonate-hosted Zn-Pb deposits in the Maestrat Basin, eastern Spain: fluid inclusion and

isotope (Cl, C, O, S, Sr) evidence, Economic Geology. 98: 933-954.

[58]. Velasco, F., Herrero, J.M., Yusta, I. Alonso, J.A., Seebold, I. and Leach, D. (2003). Geology and geochemistry of the Reocín Zinc-Lead deposit, Basque-Cantabrian Basin, northern Spain, Economic Geology. 98: 1371-1396.

[59]. Nelson, J., Paradis, S., Christensen, J. and Gabites, J. (2002). Canadian Cordilleran Mississippi Valley-Type Deposits. A Case for Devonian-Mississippian Back-Arc Hydrothermal Origin, Economic Geology. 97: 1013-1036.

[60]. Large, R.R. Bull, S. Winefield, R.W. (2001). Carbon and Oxygen Isotope Halo in Carbonates Related to the McArthur River (HYC) Zn-Pb-Ag Deposit, North Australia.

[61]. Wang, Ch., Zhang, D., Wu, G., Santosh, M., Zhang, J., Xu, Y. and Zhang, Y. (2014). Geological and isotopic evidence for magmatic-hydrothermal origin of the Ag–Pb–Zn deposits in the Lengshuikeng District, east-central China, Mineralium Deposita. 49: 733-749.

[62]. Xiong, S.F., Gong, Y.J., Jiang, S.Y., Zhang, X.J., Li, O. and Zeng, G.P. (2018). Ore genesis of the Wusihe carbonate-hosted Zn-Pb deposit in the Dadu River Valley district, Yangtze Block, SW China: evidence from ore geology, S-Pb isotopes, and sphalerite Rb-Sr dating, Mineralium Deposita. 53: 967-979.

[63]. Rajabi, A. Rasta, E. Canet, C. and Alfonso, P. (2015). The early Cambrian Chahmir shale-hosted Zn–Pb deposit, Central Iran: an example of vent-proximal SEDEX mineralization, Mineralium Deposita. 50: 571-590.

[64]. Gadd, M.G. Mattews, D.L. Peter, J.M. and Jansson, I.R. (2017). The world-class Howard's Pass SEDEX Zn-Pb district, Selwyn Basin, Yukon. Part II: the roles of thermochemical and bacterial sulfate reduction in metal fixation, Mineralium Deposita. 52: 405-419.

[65]. Stöcklin, J. (1968). Structural history and tectonics of Iran: A review. American Association of Petroleum Geologists Bulletin. 52 (7): 1229–1258.

[66]. Alavi, M. (1991). Tectonic map of the Middle East (scale 1: 5, 000, 000). Geological Survey of Iran.

[67]. Annels, A.E. O'Donovan, G. and Bowles, M. (2003). New ideas concerning the genesis of the Angouran Zn–Pb deposit, NW Iran. Abstracts of the 26th Mineral Deposits Studies Group, University of Leicester, Leicester, 11–12.

[68]. Maanijou, M. (2002). Proterozoic metallogeny of Iran. Abstracts of the international symposium on the metallogeny of Precambrian shields, Kiev. 13–26.

ترکیب اطلاعات بیزین: رویکردی قابل اعتماد برای مدلسازی توصیفی ذخایر معدنی

بهزاد تخم‌چی[1*]، سوسن ابراهیمی[2]، هاله عزیزی[3]، سید رضا قوامی ریابی[1] و ناصر فرخی[4]

1- دانشکده مهندسی معدن، نفت و ژئوفیزیک، قطب مهندسی معدن، دانشگاه صنعتی شاهرود، ایران

2- دانشکده مهندسی معدن، نفت و ژئوفیزیک، دانشگاه صنعتی شاهرود، ایران

3- دانشکده مهندسی برق و علوم کامپیوتر، دانشگاه داکوتای شمالی، گرند فورکس، داکوتای شمالی، آمریکا

4- گروه بیولوژی سلولی و مولکولی، دانشکده علوم زیستی و بیوتکنولوژی، دانشگاه شهید بهشتی، تهران، ایران

ارسال 2019/1/16، پذیرش 2019/4/12

* نویسنده مسئول مکاتبات: tokhmechi@ut.ac.ir

چکیده:

شناسایی ژنز ذخایر معدنی، کماکان برای زمین‌شناسان اقتصادی یک چالش محسوب می‌شود. در این مقاله، روش ترکیب اطلاعات بیزین برای رسیدن به اطمینان بیشتری در خصوص ژنز معرفی می‌گردد و کاربرد آن در خصوص یک مسئله ساختگی برای شناسایی ژنز بر اساس وجود دو ویژگی (مس و سرب + روی) و سه ویژگی (مس، سرب + روی و نقره) مورد بررسی قرار می‌گیرد. سپس کارکرد روش در شناسایی ژنز معدن سرب و روی انگوران مورد بررسی قرار می‌گیرد. برای این معدن، در مراجع مختلف، سه ژنز معرفی شده است: ماسیو سولفاید، تیپ دره می‌سی‌سی‌پی و سدکس. بر اساس مطالعات، روش ترکیب اطلاعات بیزین در کاهش عدم قطعیت تشخیص ژنز سونگون از 50 درصد به 30 درصد مؤثر بوده است. بعلاوه، قابل اثبات است که استفاده از ویژگی‌های بیشتر در شناسایی دقیق‌تر ژنز مفید خواهد بود؛ به نحوی که انجام مطالعه بر روی داده‌های ساختگی نیز نشان داد که تفکیک ژنز در حالت استفاده از سه ویژگی به نحو مطلوب‌تری نسبت به حالت استفاده از دو ویژگی رخ داده است. همچنین در مقاله اثبات شده است که روش ترکیب اطلاعات بیزین این قابلیت را دارد که در صورت استفاده از داده‌های مراحل مختلف اکتشاف به شناسایی بهتر ژنز کمک کند.

کلمات کلیدی: ترکیب داده، پیچیدگی، تصمیم‌گیری، زمین‌شناسی اقتصادی، کاهش عدم قطعیت.